INRIA-GAMMA3 Contribution to 1st AIAA Sonic-Boom workshop

Adrien Loseille [1] and **Frédéric Alauzet**[1]

[1] EPI GAMMA3
INRIA Paris-Rocquencourt

Scope of the study

Inviscid cases only

69-degree Delta Wing	provided-unstructured and adaptive grids
SEEB-ALR	provided-unstructured and adaptive grids

General context

- Tetrahedral meshes only
- Parallel computation 4-core Intel Xeon @ 2.9Ghz

  simulation time $<$ 3 hours
- Error estimates

multi-scale	interpolation error	Mach number
goal-oriented	approximation error	pressure observation

Conservative Euler equations:

$$
\left\{
\begin{array}{rcl}
\dfrac{\partial \rho}{\partial t} + \nabla.(\rho \vec{U}) & = & 0\,, \\
\dfrac{\partial (\rho \vec{U})}{\partial t} + \nabla.(\rho \vec{U} \otimes \vec{U}) + \nabla p & = & 0\,, \\
\dfrac{\partial (\rho E)}{\partial t} + \nabla.((\rho E + p)\vec{U}) & = & 0\,,
\end{array}
\right.
$$

Numerical resolution: Mixed-Element-Volume Method (MEV)

- vertex-centered: low complexity
- edge-based formulation with upwind element: 1D splitting
- MUSCL type method: inexpensive high-order extensions
- Properties:
  - Conservative
  - Positivity preserving
  - Monotone: TVD

Discretization:

- Euler equation are rewritten:

$$\frac{\partial W}{\partial t} + \nabla \cdot F(W) = 0 \quad \text{where} \quad W = {}^{t}(\rho, \rho u, \rho v, \rho w, \rho E)$$

- Finite-Volume cell C_i: median cell

$$|C_i| \frac{dW_i}{dt} + \int_{\partial C_i} F(W_i) \cdot \vec{n}_i \, d\gamma = 0$$

- Integration of the convective fluxes:

$$\begin{aligned} \int_{\partial C_i} F(W_i^n) \cdot \vec{n}_i \, d\gamma &= \sum_{P_j \in \mathcal{V}(P_i)} F|_{I_{ij}} \cdot \int_{\partial C_{ij}} \vec{n}_i \, d\gamma \\ &= \sum_{P_j \in \mathcal{V}(P_i)} \Phi_{ij}(W_i, W_j, \vec{n}_{ij}) \end{aligned}$$

Numerical flux: HLLC Riemann solver

$$F_{HLLC} = \begin{cases} F_l & \text{if } S_L > 0 \\ F_l^* & \text{if } S_L \leq 0 < S_M \\ F_r^* & \text{if } S_M \leq 0 \leq S_R \\ F_r & \text{if } S_R < 0 \end{cases}$$

$$\begin{aligned} \text{with } F_l^* &= F_l + S_L(U_l^* - U_l) \\ \text{and } F_r^* &= F_r + S_R(U_r^* - U_r) \end{aligned}$$

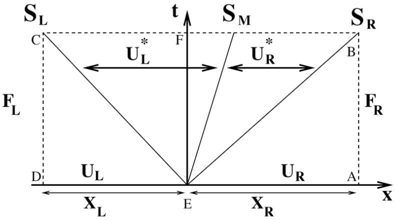

with appropriate contact and acoustic wave speeds based on Roe average we have:

- exact resolution of isolated contact
- exact resolution of isolated shock
- positivity preservation

Spatial high-order: MUSCL type method

- Use extrapolated values W_{ij} and W_{ji} of W at the interface ∂C_{ij}

$$\Phi_{ij} = \Phi_{ij}(W_{ij}, W_{ji}, \vec{\nu}_{ij}) \quad \text{with}$$

$$\begin{cases} W_{ij} = W_i + \dfrac{1}{2} (\nabla W)_{ij} \cdot \overrightarrow{P_i P_j} \\ W_{ji} = W_j + \dfrac{1}{2} (\nabla W)_{ji} \cdot \overrightarrow{P_j P_i} \end{cases}$$

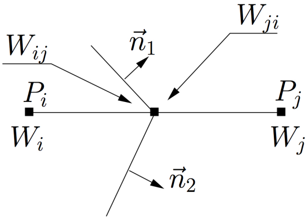

- High-order gradient: $(\nabla W)_{ij}^{HO} = 2/3\,(\nabla W)_{ij}^{C} + 1/3\,(\nabla W)_{ij}^{D}$

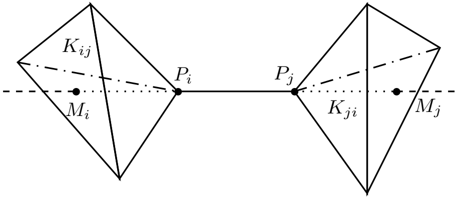

Spatial limited high-order:

- this approach leads to a third-order scheme for linear advection on structured simplicial meshes
- but this scheme is not monotone $\Longrightarrow$ requires a limiting process
- generalization of the SuperBee Limiter with three entries:

$$\begin{cases} Lim(u,v,w) = 0 & \text{if } uv \leq 0 \\ Lim(u,v,w) = Sign(u)\, min(2\,|u|, 2\,|v|, |w|) & \text{else} \end{cases}$$

and practically:

$$Lim((\nabla W)_{ij}^{C}, (\nabla W)_{ij}^{D}, (\nabla W)_{ij}^{HO})$$

Time advancing: matrix-free implicit LUSGS or SGS scheme

Linearized system reads:

$$\mathbf{A}\,\delta\mathbf{W}^n = \mathbf{R}^n$$

$$\text{where} \quad \mathbf{A} = \frac{V}{\delta t}\mathbf{I} - \frac{\partial \mathbf{R}^n}{\partial \mathbf{W}} \quad \text{and} \quad \delta\mathbf{W}^n = W^{n+1} - W^n$$

This system can be re-written:

$$(\mathbf{D}+\mathbf{L})\mathbf{D}^{-1}(\mathbf{D}+\mathbf{U})\,\delta\mathbf{W}^n = \mathbf{R}^n + (\mathbf{L}\mathbf{D}^{-1}\mathbf{U})\,\delta\mathbf{W}^n$$

The following approximate system is used:

$$(\mathbf{D}+\mathbf{L})\mathbf{D}^{-1}(\mathbf{D}+\mathbf{U})\,\delta\mathbf{W}^n = \mathbf{R}^n\,.$$

Matrix $(\mathbf{D}+\mathbf{L})\mathbf{D}^{-1}(\mathbf{D}+\mathbf{U})$ is inverted in two sweeps:

Forward sweep: $(\mathbf{D}+\mathbf{L})\,\delta\mathbf{W}^* = \mathbf{R}$

Backward sweep: $(\mathbf{D}+\mathbf{U})\,\delta\mathbf{W} = \mathbf{D}\delta\mathbf{W}^*$

Anisotropic Error estimates

Interpolation error controlled:

Observation solution field:

Mach number : u_h $\Longrightarrow$ control of $\|R_h(u_h) - \Pi_h R_h(u_h)\|_{\mathbf{L}^2(\Omega)}$

Anisotropic goal-oriented

Observation functional:

$$j(U) = \int_S (p - p_\infty)^2 \quad \Longrightarrow \quad \text{control of} \quad |j(U) - j_h(U_h)|$$

S is the outer domain boundary:

- half-space $\theta \in [0, 90]$ for the delta-wing
- $\theta \in [0, 90]$ for the seeb.

Local remeshing : Feflo.a

- surface and volume remeshing
- metric-based for anisotropy

Delta-Wing case: uniform grids

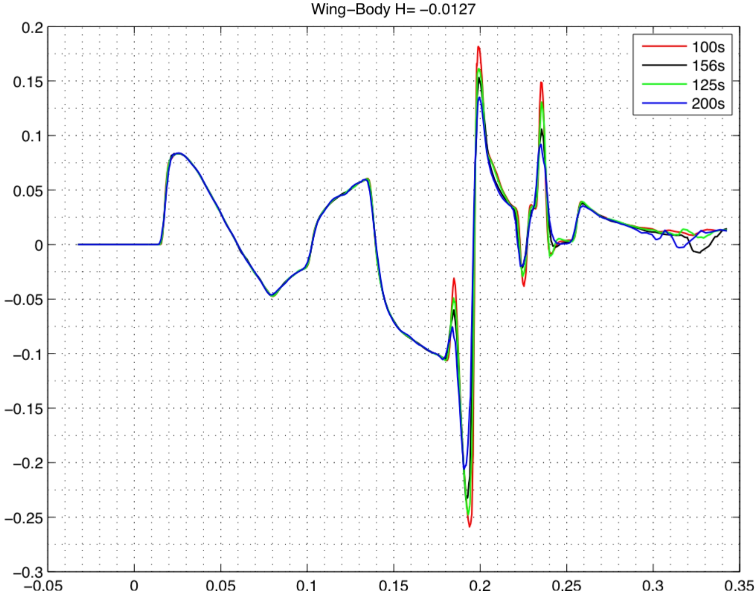

Delta-Wing case: uniform grids

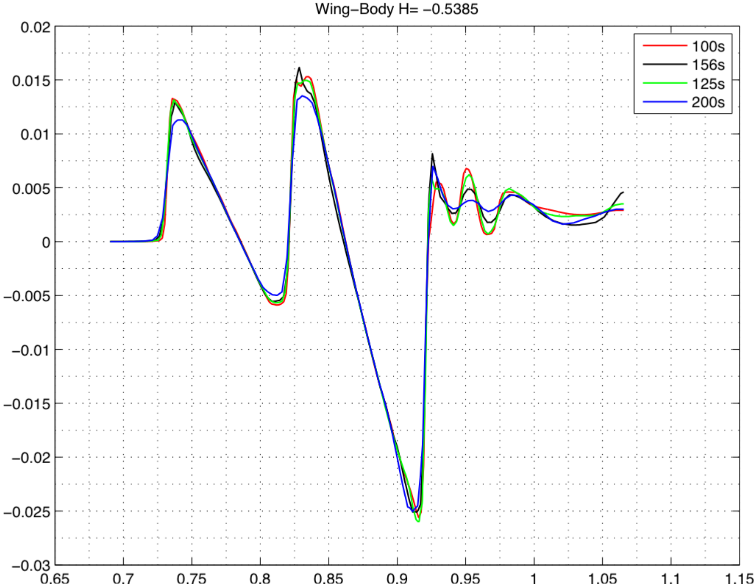

Delta-Wing case: uniform grids

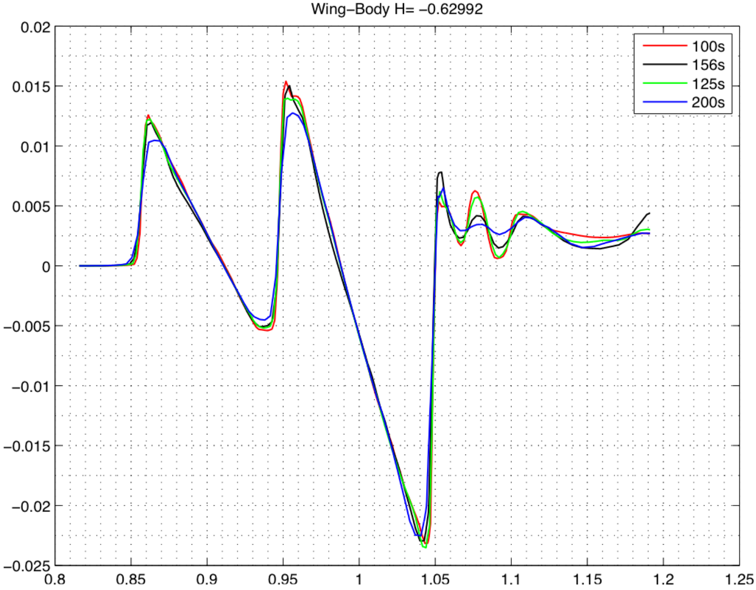

Delta-Wing case: uniform grids

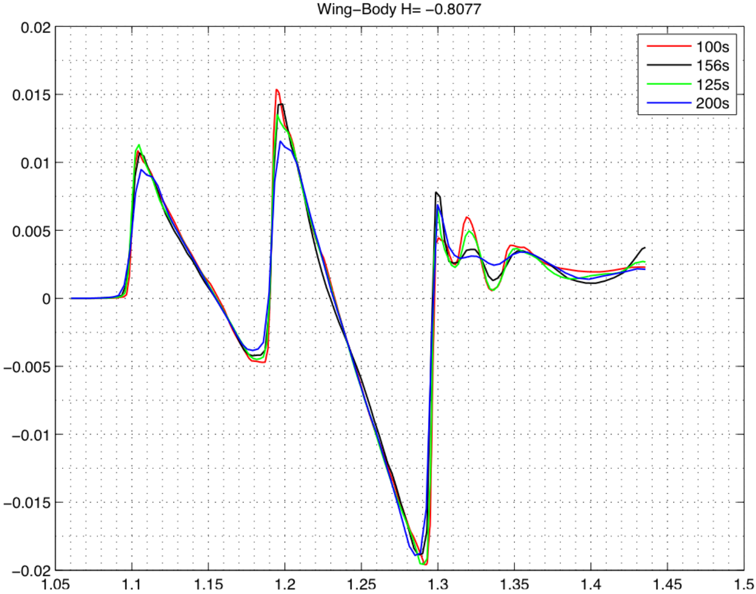

Delta-Wing case: adaptive grids

Adjoint-based mesh adaptation:

- 30 adaptations, $\approx$26000 solver iterations in total
- Cpu time $<$ 3 hours
- Max cpu time for one iteration:
  - Error estimate 1 min,
  - Remeshing 6 min
  - Flow 10 min

# vertices	# tetrahedra	mean ratio	mean quotient
28744	156978	18	237
52641	295102	21	360
101937	580593	24	491
198086	1140680	27	672
384684	2233859	30	856
759048	4433632	34	1063

Similar strategies/observations for multi-scale mesh adaptation

Delta-Wing case: adaptive grids

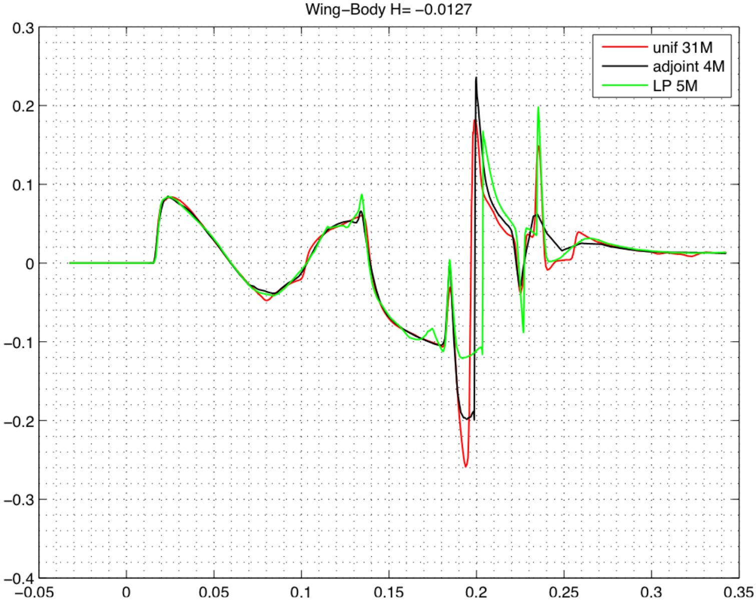

Delta-Wing case: adaptive grids

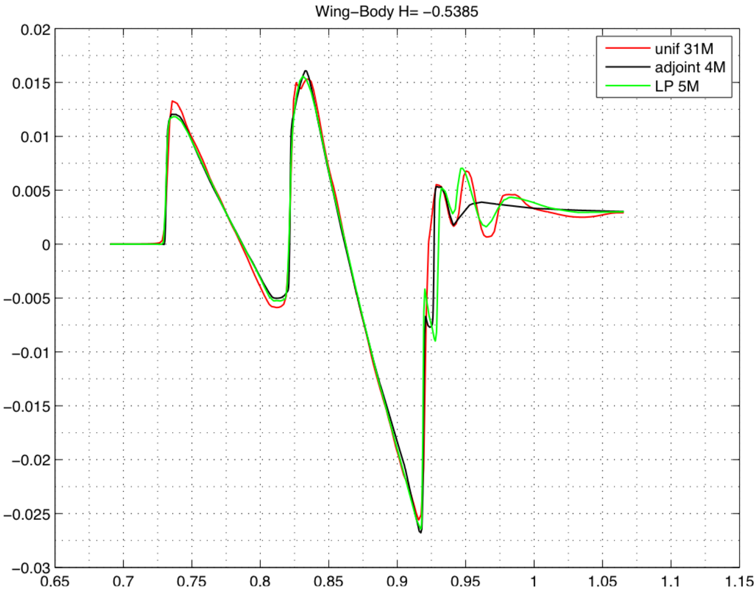

Delta-Wing case: adaptive grids

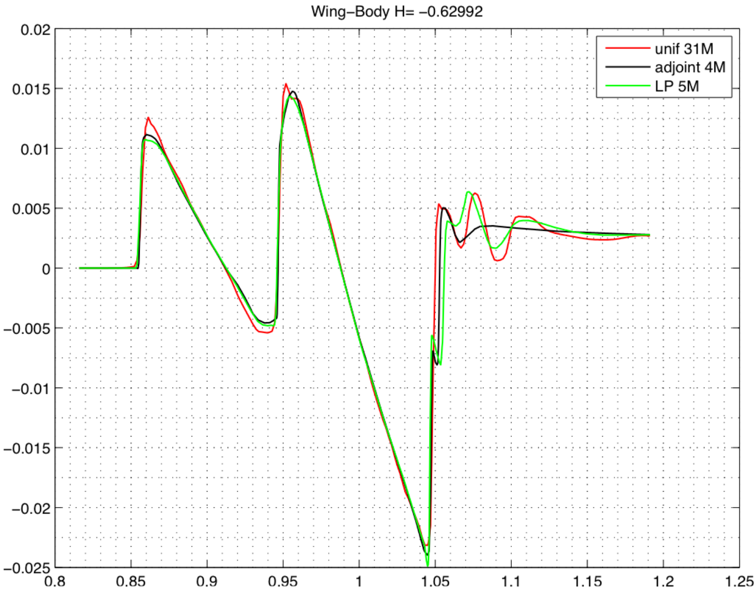

Delta-Wing case: adaptive grids

Delta-Wing case: adaptive grids

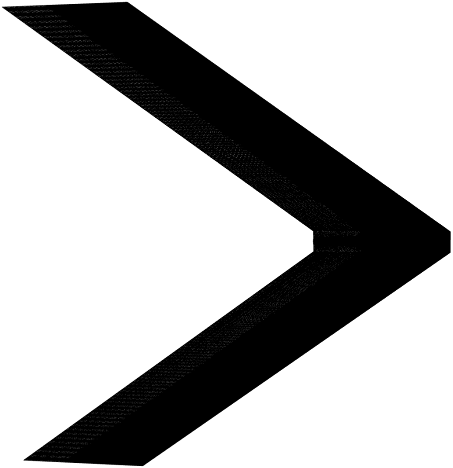

Uniform 31M

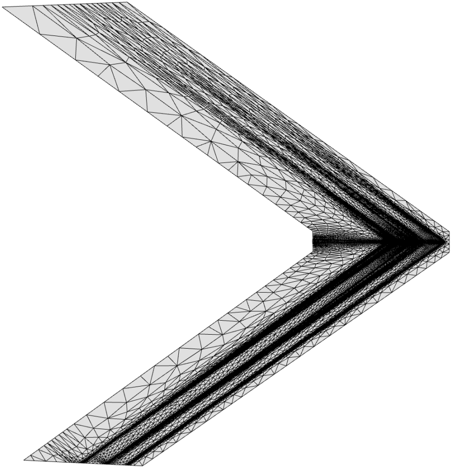

Adjoint 4M

Delta-Wing case: adaptive grids

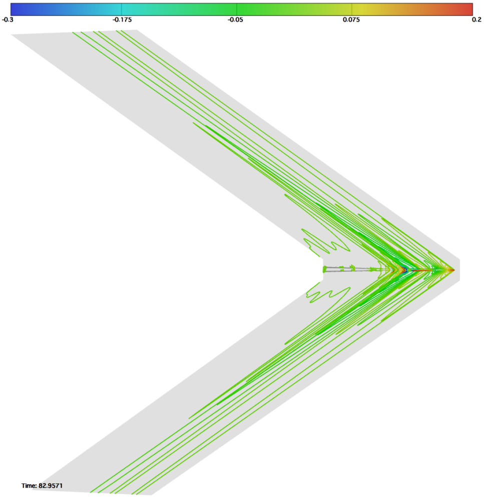

Uniform 31M

Adjoint 4M

Delta-Wing case: adaptive grids

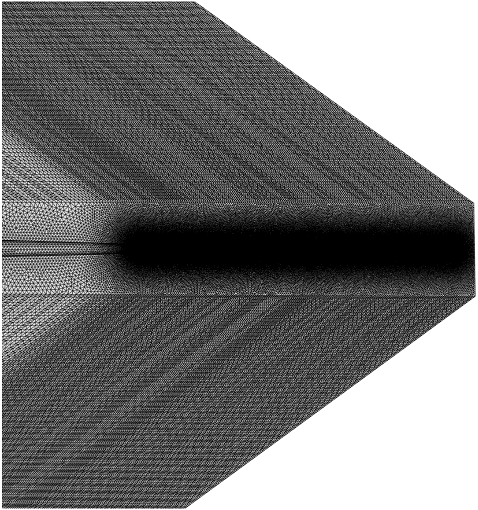

Uniform 31M

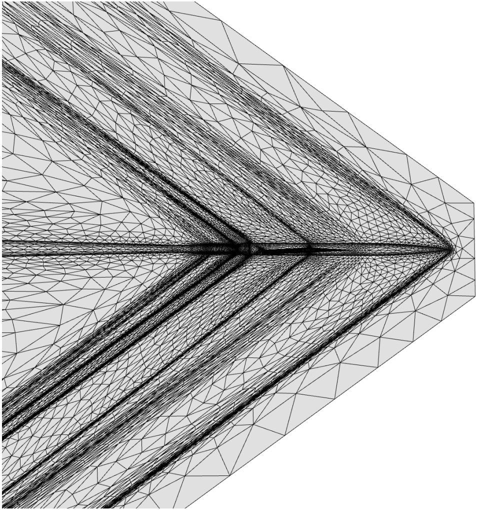

Adjoint 4M

Delta-Wing case: adaptive grids

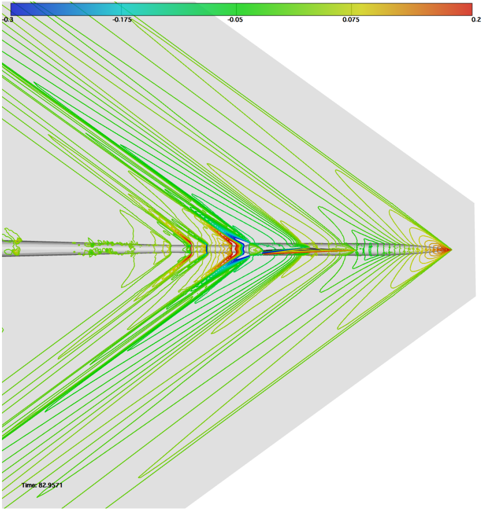

Uniform 31M

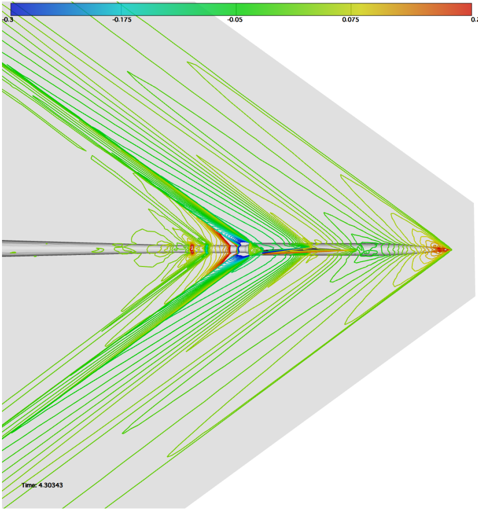

Adjoint 4M

Delta-Wing case: adaptive grids

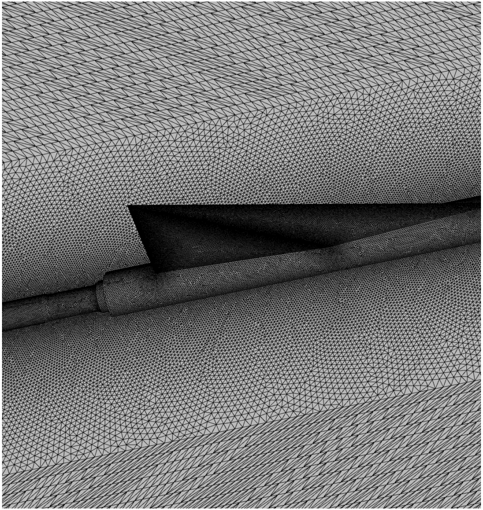

Uniform 31M

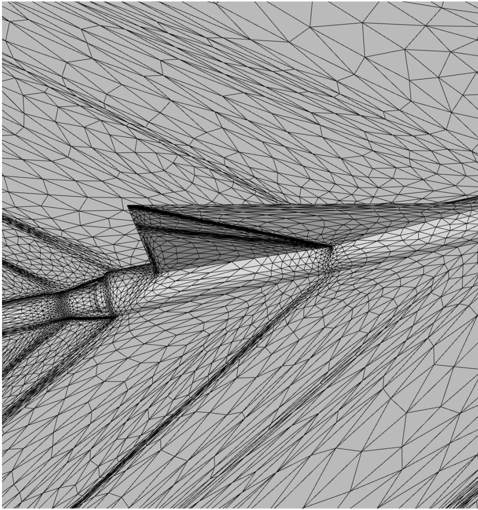

Adjoint 4M

Delta-Wing case: adaptive grids

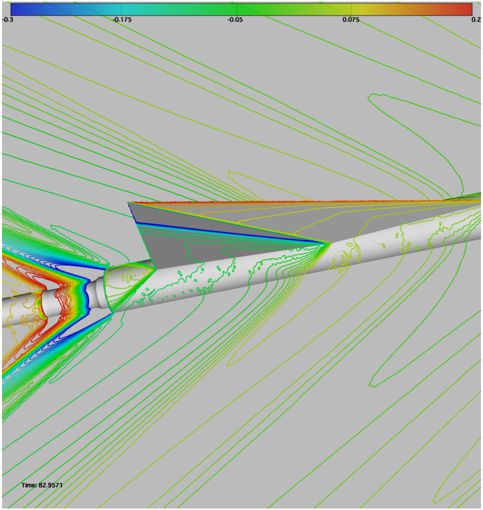

Uniform 31M

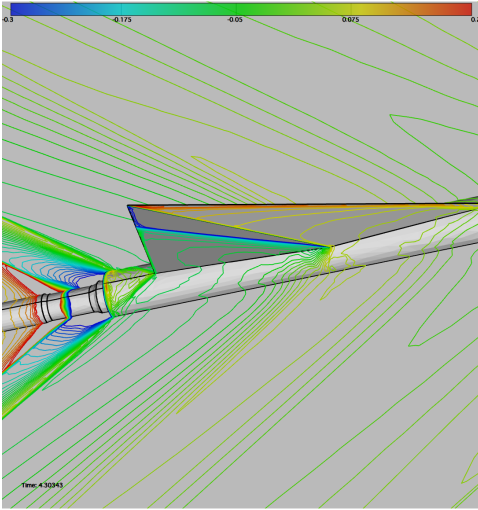

Adjoint 4M

SEEB-ALR case: uniform grids

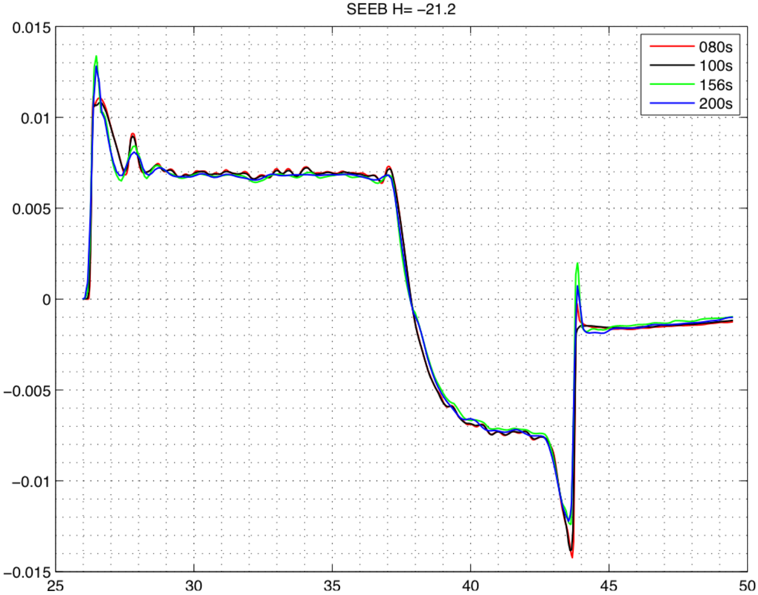

SEEB-ALR case: uniform grids

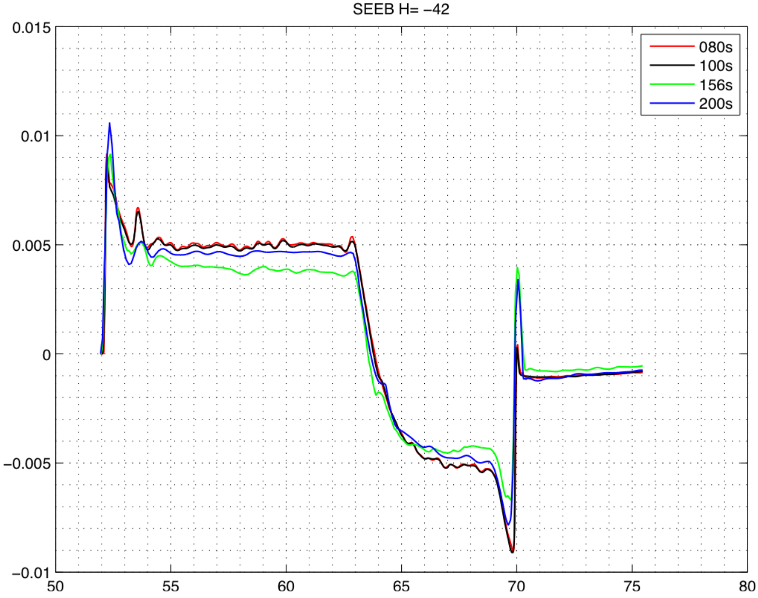

Adjoint-based mesh adaptation:

- 25 adaptations, ≈22000 solver iterations in total
- Cpu time $<$ 2 hours
- Max cpu time for one iteration:
  - Error estimate 20 sec,
  - Remeshing 3 min
  - Flow 10 min

# vertices	# tetrahedra	mean ratio	mean quotient
13701	68911	10	80
26448	140256	15	195
50310	275468	21	415
97849	547182	25	589
196130	1112418	28	727

SEEB-ALR case: adaptive grids

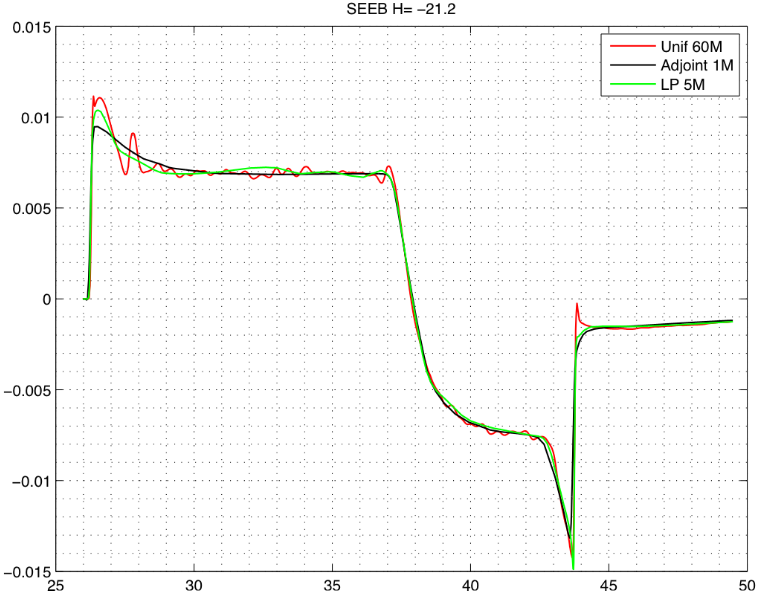

SEEB-ALR case: adaptive grids

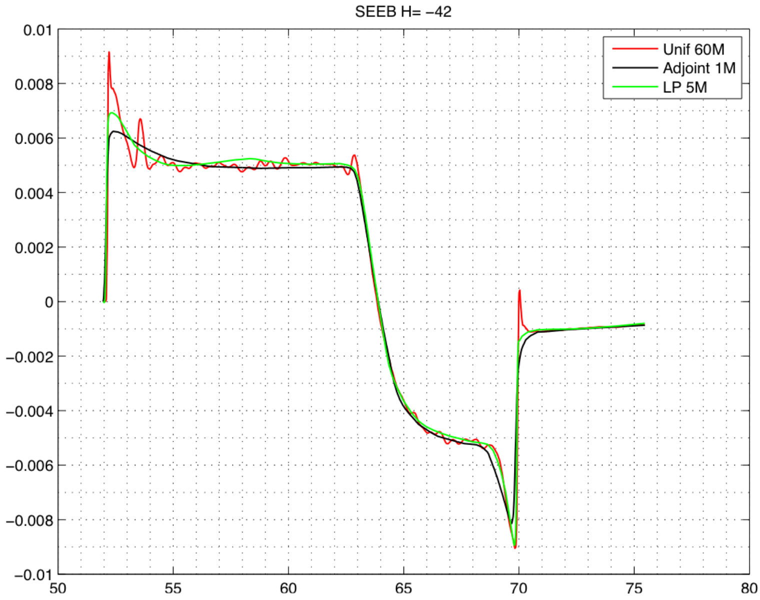

SEEB-ALR: adaptive grids

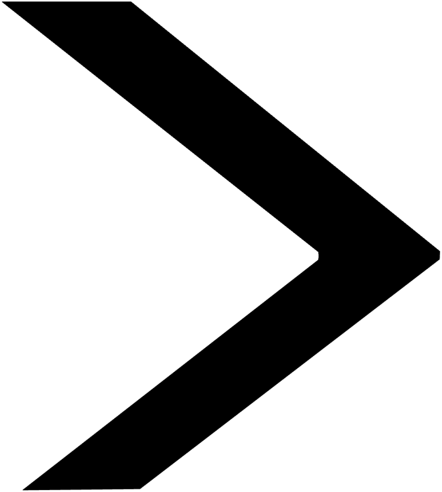

Uniform 60M

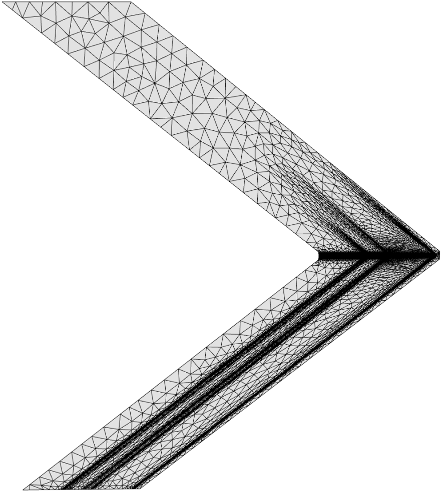

Adjoint 1M

SEEB-ALR: adaptive grids

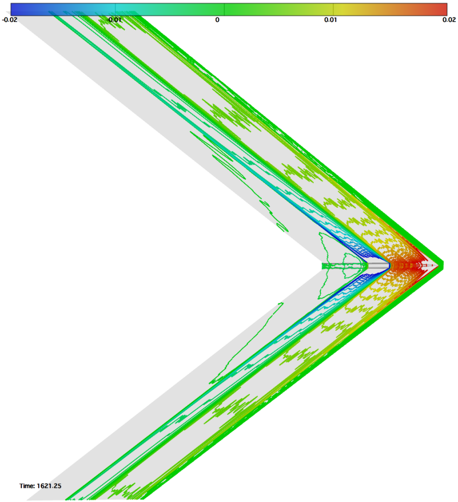

Uniform 60M

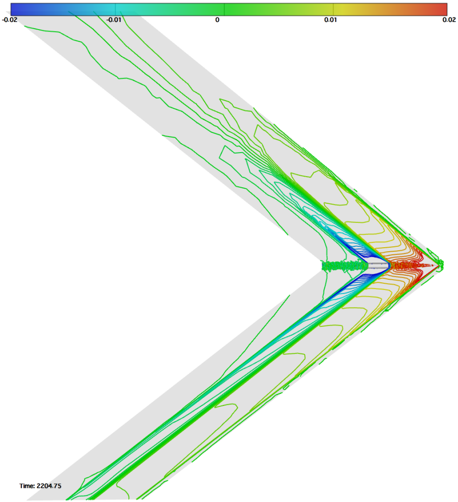

Adjoint 1M

SEEB-ALR: adaptive grids

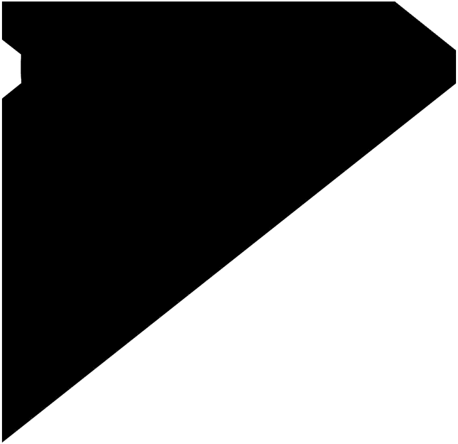

Uniform 60M

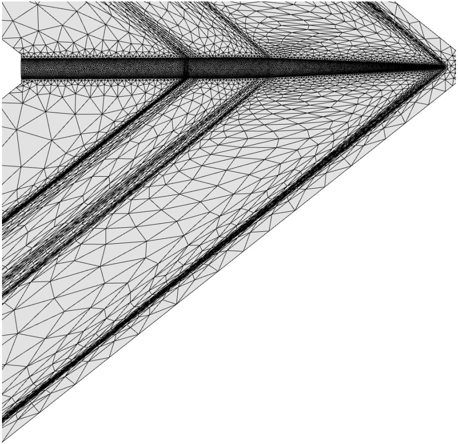

Adjoint 1M

SEEB-ALR: adaptive grids

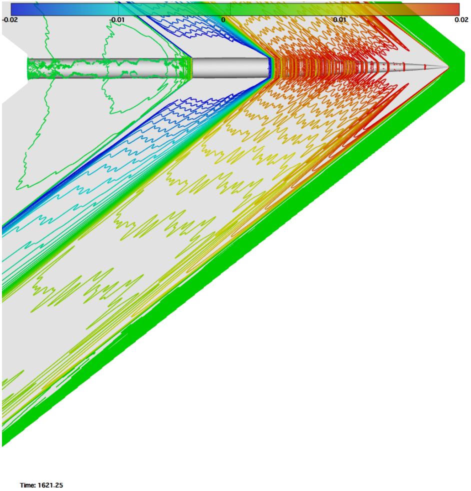

Uniform 60M

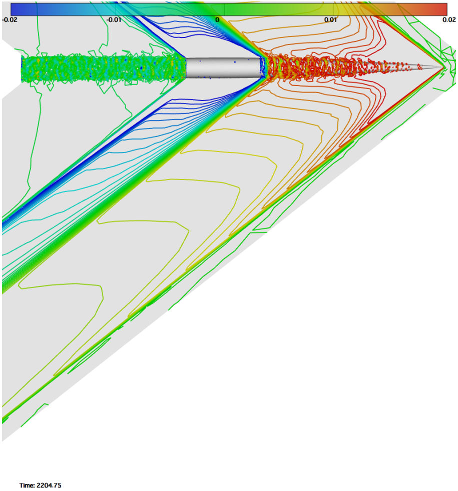

Adjoint 1M

Concluding remarks : solver

- Solver convergence on adaptive meshes :
  - Small unsteadiness appears behind the body
  - Cycles appear in the residual $\Longrightarrow$ freezing of high-order gradients

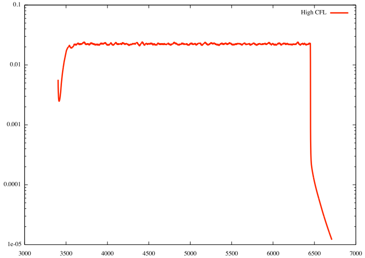

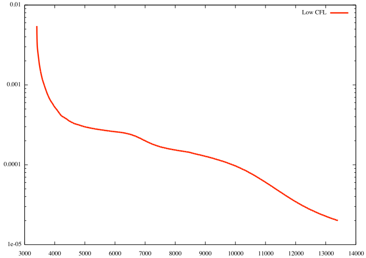

Concluding remarks : solver

- Sensitivity to the mesh:
  - Oscillations (on surface/volume) induced by the discrete mesh ?
  - Use (CAD,exact) normals to compute boundary fluxes

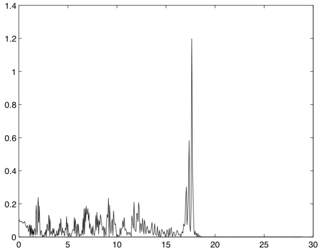

Concluding remarks : adaptation

- Adjoint observed only at the largest R/L
  - Only observed-signal is converged
  - Local strong non-linearities at small R/L have little impact at signal at large R/L

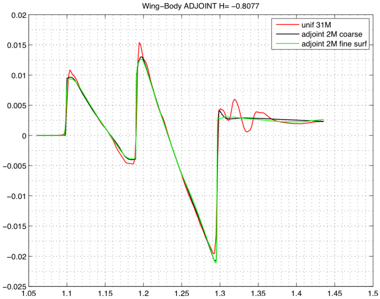

Delta-wing case